

## Hydration of Ca-montmorillonite at basin conditions: A Monte Carlo molecular simulation

**Raúl Monsalvo<sup>1</sup>, Liberto de Pablo<sup>2,\*</sup>, and M. Lourdes Chávez<sup>1</sup>**

<sup>1</sup> Facultad de Química, Universidad Nacional Autónoma de México, Ciudad Universitaria, Circuito Interior, Del. Coyoacán, 04510 México, D. F., Mexico.

<sup>2</sup> Instituto de Geología, Universidad Nacional Autónoma de México, Ciudad Universitaria, Circuito Exterior, Del. Coyoacán, 04510 México, D. F., Mexico.

\* liberto@servidor.unam.mx

### ABSTRACT

Monte Carlo simulations in  $NP_{zz}T$  and  $\mu VT$  ensembles of the hydration of Wyoming-type Ca-montmorillonite have shown the interlayer configurations. Ca-montmorillonite may hydrate to one-, two- and three-layer hydrates of  $d_{001}$  spacing 11.83, 13.73, and 15.60 Å at 353 K and 625 bar. At lower temperatures and pressures the spacing increases. Grand canonical simulations show that the one-layer Ca-montmorillonite hydrate of  $d_{001}$  spacing 12.11 Å is stable at 353 K, 300 bar, -7.21 kcal/mol potential, at a 2.0 km depth of normally compacted sediments. Two- and three-layer hydrates do not form. At 353 K, 625 bar, -5.58 kcal/mol potential, the one-layer hydrate is nearly stable. In the clay interlayer, the water molecules are clustered on the midplane, with their protons pointing towards the siloxane surfaces on both sides and on the midplane. The  $Ca^{2+}$  cations are solvated in outer-sphere coordination, separated 2.77 Å from the water molecules. In sedimentary basins under normal geotherms, one-layer Ca-montmorillonite is the single hydrate stable at 2 km depth; under over-compacted sediments at 2.7 km depth it becomes unstable.

Key words: montmorillonite, Ca-montmorillonite, hydration, simulation, Monte Carlo, stability.

### RESUMEN

Simulaciones Monte Carlo en conjuntos  $NP_{zz}T$  y  $\mu VT$  de la hidratación de Ca-montmorillonita tipo Wyoming muestran la configuración interlaminar. Ca-montmorillonita puede formar hidratos de una, dos y tres capas, con espaciamiento  $d_{001}$  de 11.83, 13.73, y 15.60 Å respectivamente a 353 K y 625 bar. A temperaturas menores el espaciamiento es mayor. Simulaciones en conjuntos  $\mu VT$  indican la formación del hidrato de una capa, estable a 333 K, 300 bar, potencial -7.21 kcal/mol, espaciamiento  $d_{001}$  12.11 Å. No se forman los hidratos de dos y tres capas. A 353 K, 625 bar, potencial de -5.58 kcal/mol, el hidrato de una capa no es estable. En el espacio interlaminar, las moléculas de agua se agrupan en el plano intermedio alternativamente orientadas con los protones hacia las superficies de siloxano a ambos lados y en el plano intermedio. Los cationes  $Ca^{2+}$  están totalmente solvatados, fuera del plano intermedio, a distancia de 2.77 Å de las moléculas de agua. En sedimentos bajo condiciones normales el monohidrato de Ca-montmorillonita es estable a 2 km de profundidad, mientras que bajo sedimentos sobre-compactados a 2.7 km de profundidad se vuelve inestable.

Palabras clave: montmorillonita, Ca-montmorillonita, hidratación, simulación, Monte Carlo, estabilidad.

## INTRODUCTION

The adsorption of fluids and chemical species by expandable clay minerals is important to diagenetic, metamorphic, petrologic, and geochemical processes (Huggett and Shaw, 1993), soil physics, properties and behavior of soils (Aylmore and Quirk, 1967), stability, retention and transport of contaminants (Cotter-Howells and Patterson, 2000), waste management (Rutherford *et al.*, 1980) and, in oil exploration and recovery, to borehole stability (Hall *et al.*, 1986; Hall, 1993), adsorption of stabilizing additives and polymers, overpressure and migration of hydrocarbons (Hall, 1993).

The hydration and dehydration of the minerals result in adsorption or separation of fluids and chemical species that affect contamination, rock strength, pore pressure, swelling, and the overall stability of clay systems. The interactions between the clays and fluids are of particular interest to the retention of nutrients and the adsorption, accumulation, decomposition, release, transport, and ultimate fate of contaminants in soils, to soil mechanics, and in petroleum-rich basins to the recovery of oil and gas and the quality of the reservoir.

Clay minerals of the smectite type are common. In soils and sediments usually occur Na-, Ca-, and Mg-montmorillonite or their combinations. In clay deposits, in Mexico are found Ca-, Na-, and Mg-montmorillonite in the underclays of the Mexican Basin, subjected to hydration-dehydration, contaminants, and occasional multiplying seismic effects; in Durango the dominant specie is Na-montmorillonite, low-calcic and high-swelling, whereas in other localities, namely Tlaxcala and Guerrero, predominate Ca- and Mg-montmorillonite.

In industrial processes, smectites are normally used in their protonic form or with different adsorbed metallic and organic species to impart distinct properties. Their characteristics and behavior vary, usually associated with their silicic framework and surface properties; structural replacements modify the structural framework to change the surface properties and ultimate behavior of the clay. Reactions on the clay surface define their properties. Na- and Ca-montmorillonite are the most abundant on which other chemical species, fluids, metallic and organic ions or molecules build.

Smectites are relatively stable but prone to transform and modify their properties. Their fine particle size and disordered structure are not easily amenable to some analytical techniques but they are characterized by proper mineralogical procedures. Their surface properties are highly sensitive to the surrounding environment and more complex to characterize, essentially on account of their *in situ* behavior. As in many geochemical and mineralogical processes, *i.e.*, mineral deposition from hydrothermal fluids or mineral stability at high temperatures, pressures or depths under brines and oil fluids, require complex interpretations and explanations, often distinct from those available from

experimental data or extrapolated from different environments and conditions.

In the present paper is discussed the behavior of Ca-montmorillonite under surface and low-depth environments, as determined from molecular simulations. Reactions on the clay surface are fundamental to establish interrelations with parent minerals and understanding related processes. Molecular simulations allow characterization of the clay interlamellar space at the atomic and molecular levels, identifying fundamental properties, reaction mechanisms, thermodynamics, and kinetics of reactions, mimicking *in situ* conditions not easily reproduced experimentally or where direct observation is not simple.

Ca-montmorillonite is a 2:1 expandable clay mineral that swells upon contact with water. Experimental studies (Posner and Quirk, 1964; Pezerat and Mering, 1967; Keren and Shainberg, 1975; Suquet *et al.*, 1975; McEwan and Wilson, 1980; Slade *et al.*, 1991; Sato *et al.*, 1992; Cases *et al.*, 1997; Bray *et al.*, 1998; Bray and Redfern, 1999, 2000) have shown that at the ambient conditions of 300 K and 1 bar the anhydrous phase of  $d_{001}$  spacing 9.55 – 9.96 Å hydrates to 11.19 – 12.45 Å one-layer hydrate, 15.00 – 15.50 Å two-layer hydrate, and 18.0 – 19.1 Å three-layer hydrate. Monte Carlo simulations (Chávez-Páez *et al.*, 2001a) have shown that in the same ambient environment of 300 K and 1 bar are formed stable 9.82 Å, 12.20, 14.70, and 18.4–19.0 Å anhydrous, one-, two-, and three-layer hydrates. However, the characteristics and stability of Ca-montmorillonite at conditions other than atmospheric have been scarcely described (Stone and Rowland, 1955; Koster von Groos and Guggenheim, 1987, 1989; Khitarov and Pugin, 1996; Siqueira *et al.*, 1997, 1999; Wu *et al.*, 1997; de Pablo *et al.*, 2005).

Parent Na-montmorillonite has been shown from simulation studies to form the stable monolayer hydrate at 353 K and 625 bar whereas K-montmorillonite does not (de Pablo *et al.*, 2004; Chávez *et al.*, 2004; de Pablo *et al.*, 2005). The condition of 353 K and 625 bar is particularly significant. It prevails at a 2.7 km depth of over-compacted sediments, where clay minerals may transform by adsorbing or releasing components or from reaction with circulating brines, oil and gas flows.

The behavior of the clay sediments, shales, will depend on their mineralogy, and on the temperature, pressure, and composition of the surrounding environment. Simulations studies are particularly adept considering their applicability to mimic *in situ* environments which otherwise are difficult to reproduce experimentally.

The characteristics and behavior of Ca-montmorillonite at low depths have not been described. In the present study, the stability and swelling of Wyoming-type Ca-montmorillonite are investigated by Monte Carlo simulations at constant stress in the isobaric-isothermal  $NP_{zz}T$  ensemble and at constant chemical potential in the grand canonical  $\mu VT$  ensemble, at the basin conditions of 333–353 K and 300–625 bar.

## METHODOLOGY

The hydration of Ca-saturated montmorillonite is studied by Monte Carlo simulation in the  $NP_{zz}T$  and  $\mu VT$  ensembles (Allen and Tildesley, 1987), at environments of 333 K and 300 bar existing at 2 km depth in normally compacted sediments, and of 353 K and 625 bar prevailing at 2.7 km depth of over-compacted sediments (geotherms at the Gulf of Mexico, geothermal gradient of 30 °C/km, geostatic gradient 150 bar/km, Hower *et al.*, 1976).

The simulations employ the model and approach described by Chávez-Páez *et al.* (2001a, 2001b). The clay considered is the Ca-saturated Wyoming-type montmorillonite of unit cell  $(Si_{7.75}Al_{0.25})(Al_{3.50}Mg_{0.50})O_{20}(OH)_4Ca_{0.375} \cdot nH_2O$  and charge of 0.75, 33% of which is in the tetrahedral sheet. Eight unit cells form the 320-atoms simulation cell, measuring 21.12 Å in the  $x$ -dimension, 18.28 Å in the  $y$ -dimension, and 6.56 Å in the  $z$ -dimension. The positions and charges of the atoms in the unit cell are those of pyrophyllite (Skipper *et al.*, 1995a), with substitution in the simulation cell of octahedral  $Al^{3+}$  in positions  $(-3.52, -3.05, 0)$ ,  $(7.04, -3.05, 0)$ ,  $(-3.52, 6.09, 0)$ , and  $(7.04, 6.09, 0)$  by  $Mg^{2+}$  and tetrahedral  $Si^{4+}$  in positions  $(2.64, 1.52, 2.73)$  and  $(0.88, 1.52, -2.73)$  by  $Al^{3+}$ .

The total interaction energy between atoms is defined by Equation 1, which includes the Coulomb attraction–repulsion energy and the Lennard-Jones and van der Waals dispersion energy. Chávez-Páez *et al.* (2001a) simulated the interaction energy from Equation 2, which combines the model of Skipper *et al.* (1995a, 1995b) for the clay–water system and the TIP4P water model of Jorgensen *et al.* (1983). In Equation 2, the first term of the summation represents the Coulomb attraction–repulsion contribution to the total energy of interaction whereas the remaining terms correspond to the Lennard-Jones dispersion contribution,  $m_i$  and  $m_j$  are the number of sites in molecules  $i$  and  $j$ ,  $q_{ia}$  is the charge at site  $a$  of molecule  $i$ ,  $q_{jb}$  is the charge at site  $b$  of molecule  $j$ ,  $r_{iajb}$  is the distance between atom  $a$  in molecule  $i$  and atom  $b$  in molecule  $j$ . The parameters  $A$ ,  $B$ ,  $C$ ,  $D$ ,  $E$ ,  $F$ , and  $G$  are site specific parameters developed for the interaction between calcium and TIP4P water. In the present case the parameters of Bounds (1985) (Table 1) are used.

$$U_{ij} = U_{ij}^{Coul} + U_{ij}^{LJ} \quad (1)$$

$$U_{ij} = \sum_{a=1}^{m_i} \sum_{b=1}^{m_j} \left[ \frac{q_{ia} \cdot q_{jb}}{r_{iajb}} - A_{iajb} \cdot e^{-B_{iajb} \cdot r_{iajb}} + C_{iajb} \cdot e^{-D_{iajb} \cdot r_{iajb}} + \frac{E_{iajb}}{(r_{iajb})^{12}} - \frac{F_{iajb}}{(r_{iajb})^6} - \frac{G_{iajb}}{(r_{iajb})^4} \right] \quad (2)$$

In constant stress simulation,  $NP_{zz}T$ , the stress  $P_{zz}$  normal to the clay surface, the temperature  $T$ , and the number

of molecules  $N$  are kept constant. The system is allowed to sample the configuration space through molecular displacements and volume fluctuations. Volume fluctuations are allowed only in the direction normal to the clay surface. The acceptance probability of a new configuration  $n$  generated from a configuration  $m$  by displacing an atom or by changing the volume of the simulation box is given by Equation 3.

$$P_{acc} = \min \left( 1, \exp \left( -\beta \cdot \left[ \Delta U_{nm} + P_{zz} \cdot \Delta V_{nm} - \frac{N}{\beta} \cdot \ln \left( \frac{V_n}{V_m} \right) \right] \right) \right) \quad (3)$$

$\Delta U_{nm}$  is the difference in energy between the two configurations,  $\Delta V_{nm}$  is the difference in volume, and  $V_n$  and  $V_m$  are the corresponding volumes,  $\beta^{-1} = k_b T$  is the inverse temperature,  $k_b$  is Boltzmann's constant and  $T$  is the absolute temperature.

In the grand canonical ensemble,  $\mu VT$ , chemical potential, volume, and temperature are kept constant. The system samples the configuration space through molecular displacements and concentration fluctuations. However, due to the high densities that water can reach in the clay interlayer, sampling can be inefficient and a biasing technique has to be implemented to improve sampling. It is achieved by implementing a rotational-bias insertion method, where a water molecule is inserted randomly in the system and the selection of its orientation is biased. Trial insertions are accepted with probability

$$P_{acc} = \min \left( 1, \exp \left( -\beta \cdot \left[ \delta U_{nm} + \ln \left( \frac{zV}{N+1} \right) + \frac{1}{\beta} \cdot \ln(kP_j) \right] \right) \right) \quad (4)$$

and deletion of water molecules is accepted with probability

$$P_{acc} = \min \left( 1, \exp \left( -\beta \cdot \left[ \delta U_{nm} + \ln \left( \frac{N}{zV} \right) - \frac{1}{\beta} \cdot \ln(kP_j) \right] \right) \right) \quad (5)$$

$\delta U_{nm}$  is, like  $\Delta U_{nm}$  in Equation 3, the energy difference between the two configurations,  $P_j$  is the probability of selecting the  $j$ th orientation from  $k$  randomly generated

Table 1. Interaction parameters for Ca-montmorillonite, TIP4P water model\*.

Site	C (kcal/mol)	D (1/Å)	E (Å <sup>12</sup> kcal/mol)	F (Å <sup>6</sup> kcal/mol)	G (Å <sup>4</sup> kcal/mol)
O-O	0	0	592840.4	602.71152	0
O-Ca	37146	2.9902	0	-2185.3	1578.6
H-Ca	3.7234	3.7234	0	0	0

\*Jorgensen *et al.* (1983); Bounds (1985); Boek *et al.* (1995).

orientations;  $z = \exp(\beta\mu)/A^3$  is the activity,  $A$  is the thermal length of the molecule, and  $\mu$  is the chemical potential of bulk water (Allen and Tildesley, 1987; Chávez-Páez *et al.*, 2001a, 2001b).

We simulate the water–calcium interaction applying the TIP4P water model of Jorgensen *et al.* (1983) and the parameters of Bounds (1985) (Table 1). At 300 K and 333 bar and at 353 K and 625 bar, we prefer the TIP4P model because its influence on the density or the energy does not appear significant, and by doing so our results can be compared with those known previously on Ca-saturated montmorillonite under the surface ambient environment (Boek *et al.*, 1995; Chávez-Páez *et al.*, 2001a). The water–clay and clay–calcium interactions are neglected. The simulations required  $2 \times 10^6$  Monte Carlo steps for equilibration and, after the equilibration period, simulations proceeded for additional  $2 \times 10^6$  Monte Carlo steps, until the statistics was satisfactory and smooth calculated functions developed.

## RESULTS AND DISCUSSION

### NP<sub>zz</sub>T simulations

Simulations in the NP<sub>zz</sub>T ensemble at constant mass, pressure, and temperature indicate that at the basin conditions of 353 K and 625 bar the adsorption of 32 water molecules per layer of Ca-montmorillonite (98 mg/g of clay) results in the formation of the one-layer hydrate of  $d_{001}$  spacing 11.83 Å (Table 2). The water molecules are clustered on the interlayer midplane, tilted with their hydrogen atoms oriented towards the siloxane surfaces on both sides and to the midplane (Table 2, Figure 1a). The Ca<sup>2+</sup> ions are on the interlayer midplane solvated in outer-sphere complexes, but some are closer to the clay surface. A distance of 1.624 Å separates the outmost proton layers. The configuration is illustrated in the snapshot of Figure 2a.

The adsorption of 64 molecules (196 mg/g) increases the  $d_{001}$  spacing to 13.73 Å, placing the water molecules in two well-defined layers, one to each side of the interlayer midplane, 1.899 Å apart (Table 2, Figure 1b). The water protons are distributed over four layers, two outmost ones, 3.449 Å apart, and two closer to the central plane. Ca<sup>2+</sup> ions are solvated in both layers of water, slightly off the oxygen atoms; none are midway between the two layers of water, nor are they closer to the clay surface or in inner-sphere coordination with the siloxane oxygens (Figure 2b). At higher contents of water, namely 96 molecules (294 mg/g), the spacing increases to 15.60 Å, preserving the 2-layer configuration with the water molecules separated 3.524 Å, the outmost protons 5.399 Å apart, and minor excess water molecules located about the interlayer midplane (Table 2, Figure 1c). The Ca<sup>2+</sup> ions are on the interlayer midplane and in-between the two water layers, with few atoms closer to the siloxane surface.

The results indicate that, at 353 K and 625 bar, the adsorption of 32, 64, and 96 water molecules places the molecules respectively at 0.012, 0.912–0.987, and 1.787–1.737 Å from the interlayer midplane. The interlayer configuration changes from one-layer when adsorption is between 32 and near 64 water molecules to two-layer when increased to 64–96 molecules. The Ca<sup>2+</sup> ions are essentially in outer-sphere complexes in the water layers, symmetrical to the protons and slightly off the oxygen atoms.

At 333 K and 300 bar, prevailing at 2 km depth, the adsorption of 50 water molecules develops a one-layer hydrate of  $d_{001}$  spacing 12.11 Å, higher than that formed at 353 K and 625 bar. It has water molecules off the interlayer midplane, closer to the clay surface (Table 2). Its snapshot (Figure 2c) illustrates a bulkier interlayer relative to that at 353 K when 32 molecules were adsorbed (Figure 2a).

Our simulated  $d_{001}$  spacing of 11.83 and 12.11 Å for the one-layer hydrates at 353 K and 625 bar and at 333 K and 300 bar are within the range of 11.19–12.45 Å known from experimental studies (McEwan and Wilson, 1980; Bray and Redfern, 1999, 2000) and are shorter than the 12.20 Å simulated for Ca-montmorillonite under surface conditions of 300 K and 1 bar (Laird *et al.*, 1995; Laird, 1996; Chávez-Páez *et al.*, 2001a) (Table 3). The simulated

Table 2. Monte Carlo simulation of hydrated Ca-montmorillonite, NP<sub>zz</sub>T ensemble.

Simulation	1	2	3	4
Temperature (K)	353	353	353	333
Pressure (bar)	625	625	625	300
Clay layers	2	2	2	2
Ca (atoms/cell)	3	3	3	3
Water (molecules/cell)	32	64	96	50
Water (mg/g clay)	98	196	294	153
$d_{001}$ spacing (Å)	11.83	13.73	15.6	12.11
Density (g/ml)	0.21	0.36	0.47	0.32
Energy interaction (kcal/mol)	-24.245	-19.664	-17.714	-23.36
Energy Lennard-Jones (kcal/mol)	-26.369	-13.167	-7.648	-18.609
Energy Coulomb (kcal/mol)	1.415	-6.679	-10.137	-4.75
$r_{CaO}$ 1st coordination shell (Å)	2.775	2.815	...	2.775
$g(r)$ coordination probability	10.026	7.441	...	7.906
$r_{CaO}$ 2nd coordination shell (Å)	4.715	4.71	...	4.665
$g(r)$ coordination probability	1.804	1.71	...	1.432
Water (layers/cell)	1	2	2	1
O <sup>2-</sup> distance to midplane (Å)	-0.012	-0.912	-1.787	0.012
"	...	0.987	1.737	-1.081
O <sup>2-</sup> outmost distance (Å)	0	1.899	3.524	0.91
H <sup>+</sup> distance to midplane (Å)	-0.812	-1.712	-2.687	-0.963
"	-0.012	-0.312	-1.512	0.062
"	0.812	0.362	1.562	0.927
"	...	1.737	2.712	...
H <sup>+</sup> outmost distance (Å)	1.624	3.449	5.399	1.89
Ca <sup>2+</sup> distance to midplane (Å)	-0.012	-1.087	-2.062	-0.086
"	0.787	1.137	-0.662	0.961
"	...	1.737	-0.012	...
"	...	...	0.787	...
"	...	...	2.712	...

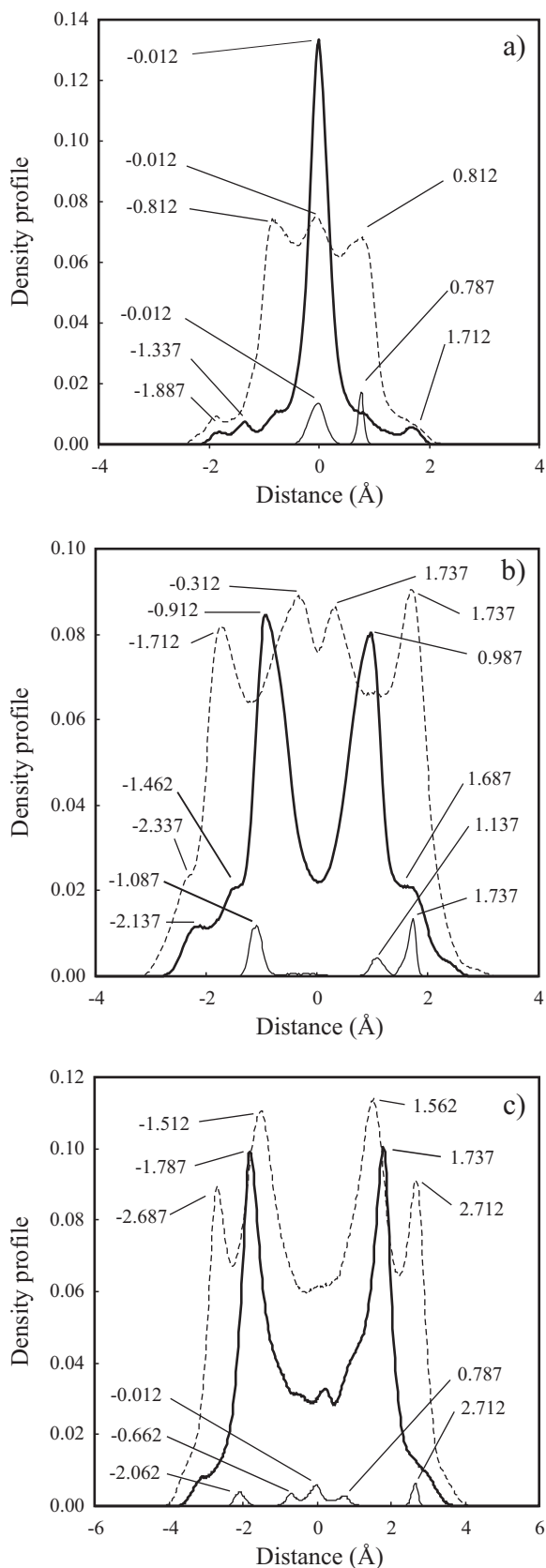


Figure 1. Density profiles of hydrated Ca-montmorillonite,  $NP_{zz}T$  ensemble. Adsorbed water molecules per simulation cell at 353 K and 625 bar are: a) 32, b) 64, c) 96. Bold line: water oxygen; dashed: protons; black: calcium.

15.60 Å spacing limiting the two-layer hydrate, with 96 adsorbed molecules of water, compares with the experimental 15.0–15.8 Å (Posner and Quirk, 1964; Keren and Shainberg, 1975; Sato *et al.*, 1992; Bray *et al.*, 1998), the 15.0 Å measured at 260–300 K and 48–7075 bar (Wu *et al.*, 1997), and the 14.7 Å (Chávez-Páez *et al.*, 2001a) known from simulations at 300 K and 1 bar. The reported three-layer hydrates of 18.50–19.10 Å spacing (Posner and Quirk, 1964; Suquet *et al.*, 1975; Sato *et al.*, 1992; Wu *et al.*, 1997; Chávez-Páez *et al.*, 2001a) were not simulated in the present work.

The radial distribution function  $g(r)$  shows for the one-layer Ca-montmorillonite hydrate a coordination probability of 10.026 molecules of water per cation, at a Ca–O separation of 2.775 Å (Table 2, Figures 3a and 3b). Increasing the adsorption to the two-layer hydrate state raises the separation to 2.815 Å and reduces the probability to 7.441. When

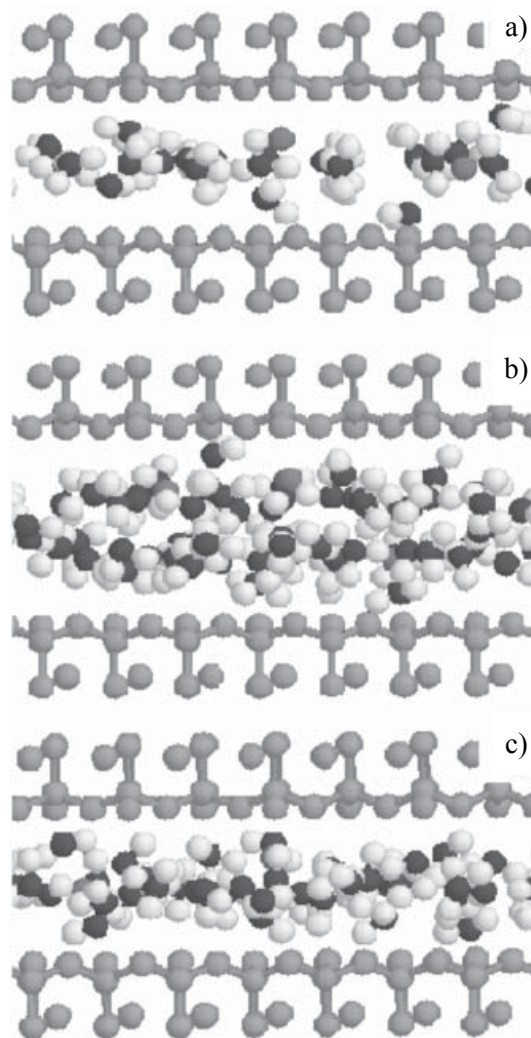


Figure 2. Snapshots of Ca-montmorillonite: a) one-layer hydrate, 32 adsorbed water molecules at 353 K and 625 bar; b) two-layer hydrate, 64 water molecules; c) one-layer hydrate, 50 water molecules at 333 K and 300 bar.

Table 3. Experimental and simulation  $d_{001}$  spacings of Ca-montmorillonite at 300 K and 1 bar.

	$d_{001}$ spacing			
Posner and Quirk (1964)	...	...	15.5	18.5
Glaeser and Mering (1968)	...	...	15.0 – 15.50	...
Suquet <i>et al.</i> (1975)	...	...	...	19.1
Keren and Shainberg (1975)	...	12	15	18
Rutherford <i>et al.</i> (1980)	9.55 – 9.70	...	...	...
Anderson <i>et al.</i> (1999)	...	...	15.5	18.5
Bray <i>et al.</i> (1998)	10.3	11.7	15	...
Sato <i>et al.</i> (1992)	9.76 – 9.80	11.19 – 12.45	15.24 – 15.81	...
Wu <i>et al.</i> (1997)	...	...	15	19.05
Chávez-Páez <i>et al.</i> (2001a)*	9.82	...	14.7	19
Chávez-Páez <i>et al.</i> (2001a)**	...	12.2	14.7	18.4

Experimental data. \*NP<sub>z</sub>T simulations; \*\* $\mu$ VT simulations.

temperature and pressure are decreased to 333 K and 300 bar, the probability is 7.906 with the  $r_{CaO}$  distance remaining at 2.775 Å. Integration of  $g(r)$  as per Equation 6 (Allen and Tildesley, 1987) indicates solvation of the cation by 10 water molecules, which is within the 9–10 range known for the calcium–water system (Bounds, 1985).

$$N_{CaO} = 4 \cdot \pi \cdot \frac{N_O}{V} \cdot \int_0^r g_{CaO} \cdot (r) \cdot r^2 dr \quad (6)$$

The progressive hydration of Ca-montmorillonite increases the  $d_{001}$  spacing and the separation of the water layers from the interlayer midplane (Table 2, Figure 4a). The energy of interaction between atoms increases in the order -24.245, -19.664, and -17.714 kcal/mol as the adsorbed H<sub>2</sub>O changes from 32 to 96 molecules (Table 2, Figure 4b).

The Coulomb energy decreases from 1.415 to -6.679 and -10.137 kcal/mol, inverse to the Lennard-Jones energy that increases to -26.369, -13.167, and -7.648 kcal/mol. The total interaction energy is lower for Ca-montmorillonite in the 333 K, 300 bar environment.

### Grand canonical $\mu$ VT simulations

To ascertain the thermodynamic stability of hydrated Ca-montmorillonite, simulations were conducted in the grand canonical  $\mu$ VT constant mass, volume and temperature ensemble. The simulations started by calculating the chemical potentials of bulk water for a system of 216 water molecules (Chávez-Páez *et al.*, 2001a, 2001b) at 353 K and 625 bar and at 333 K and 300 bar. For the former, the

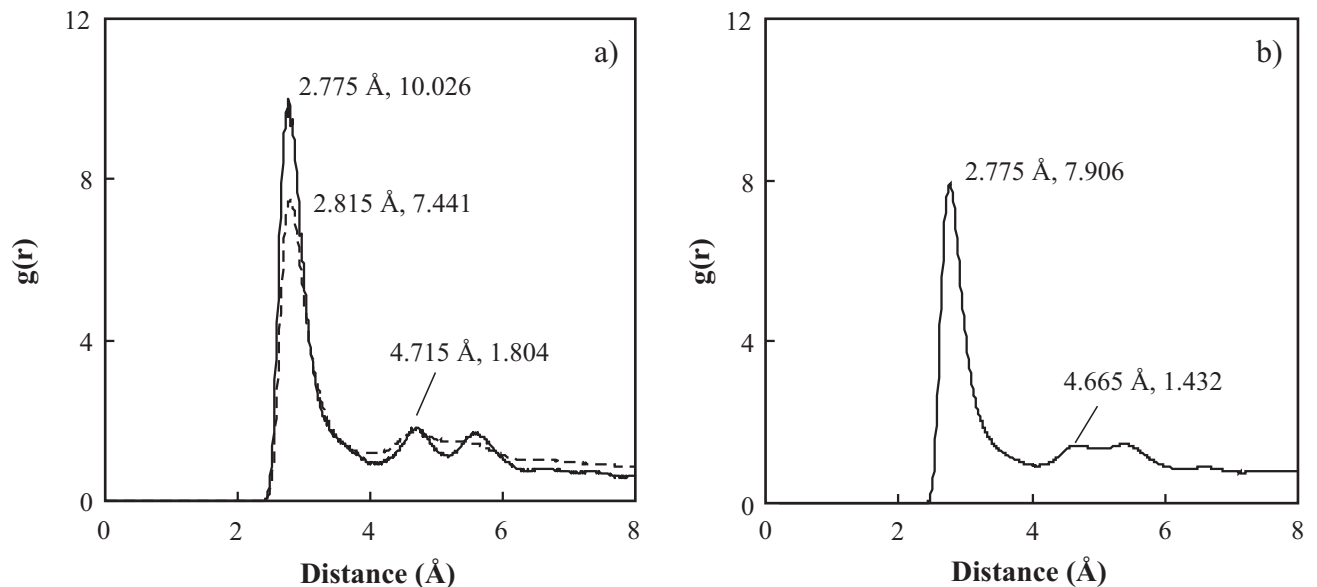


Figure 3. Radial distribution function  $g_{CaO}(r)$  of hydrated Ca-montmorillonite at: a) 353 K and 625 bar, 32 (solid line) and 64 adsorbed water molecules; b) at 333 K and 300 bar, 50 water molecules.

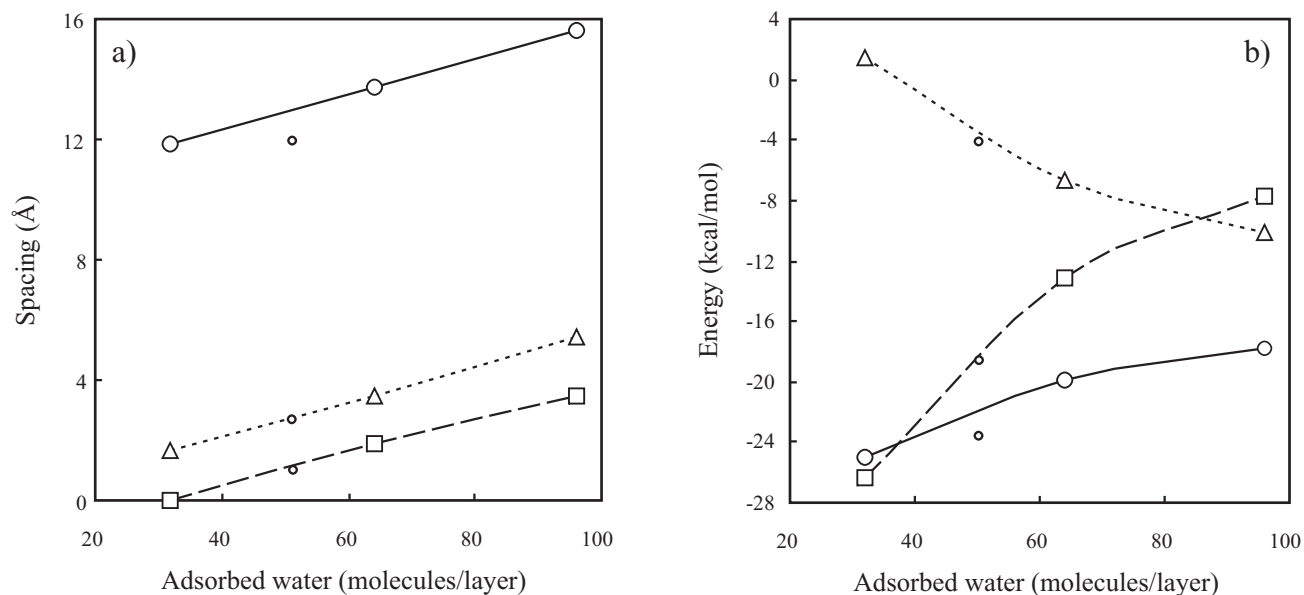


Figure 4. Hydration of Ca-montmorillonite, NP<sub>zz</sub>T ensemble, at 353 K and 625 bar. a) Change of  $d_{001}$  (o),  $H^+$  outmost separation ( $\Delta$ ),  $O^{2-}$  separation ( $\square$ ). b) Variation of the energy (o), Coulomb contribution ( $\Delta$ ), and Lennard-Jones contribution ( $\square$ ). Small circles represent the same variables at 333 K and 300 bar.

simulated chemical potential was of -5.58 kcal/mol and for the latter -7.21 kcal/mol.

Simulations in the grand canonical ensemble define the stability of the clay mineral when the chemical potentials in the mineral interlayer and of the bulk supernatant fluid are equal. The thermodynamic stability of the Ca-montmorillonite hydrates is determined from the minima in the swelling free energy as a function of the interlayer separation (Chávez-Páez *et al.*, 2001a, 2001b). The free energy is calculated from Equation 7 where  $P_{zz}$  is the interlayer pressure tensor and  $(P_{zz})^{npp}$  is the normal external bulk pressure. The derivative of this expression defines the stable  $d_{001}$  spacing when the calculated pressure tensor  $P_{zz}$  equals the bulk pressure on the clay. Values of  $P_{zz}$  distinct from the bulk pressure do not represent real solutions and lack any physical meaning; opposite assumptions would lead to collapse or blow the clay structure. A simple graphical solution is a plot depicting the dependence of  $P_{zz}$  on the  $d_{001}$  spacing.

$$\Delta E_s(\mathbf{z}) = -L_x \cdot L_y \cdot \int_0^z |P_{zz} \cdot (s) - (P_{zz})^{npp}| ds \quad (7)$$

Simulations using the TIP4P water model (Jorgensen *et al.*, 1983) show that for  $d_{001}$  spacings between 11.5 and 18 Å, the adsorbed water increases from 39.27 to 140.40 molecules per layer or 120.36 to 430.33 mg/g (Table 4, Figure 5a), the total energy changes from -22.871 kcal/mol to -16.383 kcal/mol, the Lennard-Jones energy varies from -22.116 to -3.970 kcal/mol, and the Coulomb energy from -0.601 to -12.538 kcal/mol (Figure 5b). Simulations at 333 K and 300 bar (Table 5, Figure 5c) indicate adsorption of

150.86–316.53 mg water/g,  $d_{001}$  spacing of 12.0–16.0 Å, energy of interaction -23.549 – -19.110 kcal/mol, Lennard-Jones energy -18.118 – -11.396, Coulomb energy -5.647 – -7.564 kcal/mol, and pressure tensor from 10654.69 – 2532.54 bar. The Lennard-Jones and Coulomb energies add to the total energy of interaction; the values presented in Tables 2 and 4 do not do exactly add, due to some mis-handling of the data outputs.

The variation of the pressure tensor  $P_{zz}$  with the adsorbed water depicts the path shown in Figure 6. At 353 K and 625 bar, the data in Figure 6a show that within the statistical uncertainty associated with Monte Carlo simulations, the one-layer hydrate Ca-montmorillonite approaches stability, without attain it. In the less deep environment of 333 K and 300 bar, the one-layer hydrate is stable (Figure 6b), characterized by a  $d_{001}$  spacing of 12.11 Å. Two- and three-layer hydrates do not form.

At 353 K and 625 bar, the nearly stable one-layer Ca-montmorillonite hydrate has a  $d_{001}$  spacing of 12.50 Å, formed by the adsorption of 55.21 water molecules (169.22 mg H<sub>2</sub>O/g clay), total interaction energy -21.107 kcal/mol, and interlayer density 0.342 g/mL. At 333 K and 300 bar, the stable one-layer hydrate has  $d_{001}$  12.11 Å, adsorbs 54.50 molecules of water, interaction energy -22.803 kcal/mol, Lennard-Jones dispersion -6.345 kcal/mol, Coulomb attraction–repulsion -16.449 kcal/mol, density 0.337 g/mL. The density profiles (Figure 7) show that at 353 K and 625 bar the water molecules cluster in a broad band 0.087 Å off the interlayer midplane, with protons on the midplane and 1.087 Å and 1.137 Å to each side, and the calcium cations off the midplane, solvated in outer-sphere complexes within the water layer. At 333 K and 300 bar, the density profiles

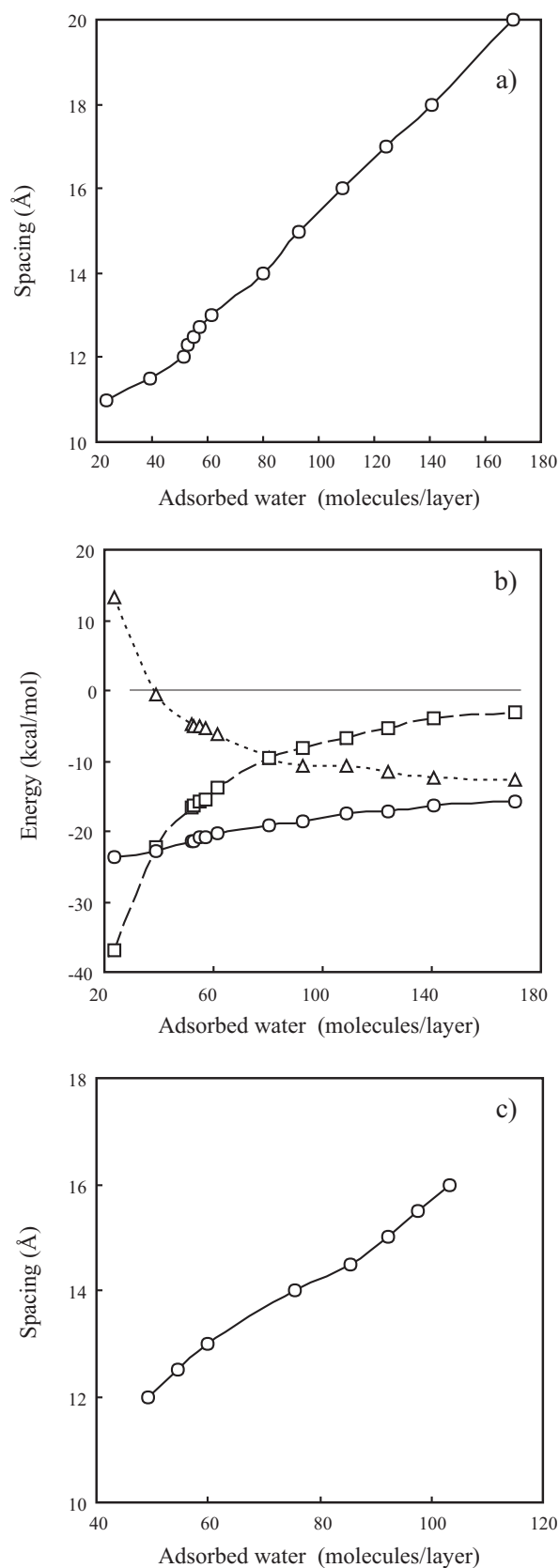


Figure 5. Effect of adsorbed water on the  $d_{001}$  spacing and the energy of Ca-montmorillonite, grand canonical  $\mu$ VT ensemble, (a) and (b) at 353 K and 625 bar, (c) at 333 K and 300 bar. Internal energy (o), Lennard-Jones contribution (□), Coulomb contribution (Δ).

indicate that the water molecules are on the interlayer midplane, oriented to both siloxane surfaces, with the protons 1.112 and 1.137 Å to both sides, slightly farther apart than at 353 K and 625 bar; the calcium atoms are solvated off the interlayer midplane. Snapshots of both hydrates (Figures 8a and 8b) show a broad layer of water molecules with the cations coordinated in the water layer, away from the siloxane surface.

Our simulations in the  $NP_{zz}T$  ensemble show that Ca-montmorillonite can form one-, two- and three-layer hydrates. Simulations in the  $\mu$ VT ensemble confirm that in normally compacted sediments at 2.0 km depth, 333 K and 300 bar, one-layer Ca-montmorillonite hydrate is stable but two- and three-layer hydrates do not form. At 353 K and 625 bar, mimicking over-compacted sediments at 2.7 km depth, the one-layer hydrate is nearly stable, not attaining full stability. In this environment, the unstable clay could transform to other minerals, adsorb from or release species to the surrounding environment to develop a stable configuration. The simulations point that Ca-montmorillonite could be stable at 353 K and 625 bar and possibly even under more stringent environments, if sediments were normally compacted or potentials more suitable.

Our results extend the stability of the one-layer Ca-montmorillonite hydrate to 2.0 km depth and probably higher, upwards from previous investigations limiting its stability to burial depths of 1.5 km, with possible conversion to other minerals in deeper environments (Siqueira *et al.*, 1997). The present simulations did not reach the high temperature and pressure of 513 K and 1200 bar (Siqueira *et al.*, 1999) and above (Wu *et al.*, 1997) experimentally determined for the stability of the 18–19 Å 3-layer hydrate and of 260–310 °C and 48–260 bar along the 0.7 g/mL isochore (Wu *et al.*, 1997) and of 453 K and 900 bar (Siqueira *et al.*, 1999) determined for its transformation to the 15 Å two-layer hydrate. Recent data from de Pablo *et al.* (2005) have confirmed that one-layer Ca-montmorillonite is stable down to 8.7 km in normally compacted sediments; two- and possibly three-layer hydrates develop at 6.7 km depth, 473 K and 1000 bar. Na- and K-montmorillonite form in similar environments one- and two-layer hydrates of  $d_{001}$  spacing larger than Ca-montmorillonite.

## SUMMARY

Monte Carlo simulations on the hydration of Ca-montmorillonite under basin-like conditions of 353 K and 625 bar and of 333 K and 300 bar reveal interlayer configurations similar to those known at the surface ambient environment of 300 K and 1 bar. At low states of hydration, the water molecules cluster on the interlayer midplane with their protons alternatively oriented towards the siloxane surfaces and on the interlayer midplane. At higher states of adsorption, the water molecules are distributed in two separate layers close to the clay surfaces, with the molecules tilted

Table 4. Monte Carlo simulation of hydrated Ca-montmorillonite,  $\mu$ VT ensemble, at 353 K and 625 bar.

Simulation	1	2	3	4	5	6	7	8	9
Temperature (K)	353	353	353	353	353	353	353	353	353
Pressure (bar)	625	625	625	625	625	625	625	625	625
Clay layers	2	2	2	2	2	2	2	2	2
Ca (atom/layer)	3	3	3	3	3	3	3	3	3
Water adsorbed (molecule/layer)	39.27	51.7	55.21	61.36	80.02	93.03	108.52	124.31	140.4
Water adsorbed (mg/g)	120.36	158.46	169.22	188.07	245.26	285.14	332.61	381.01	430.33
Spacing (Å)	11.5	12	12.5	13	14	15	16	17	18
Density (g/ml)	0.264	0.207	0.342	0.365	0.442	0.48	0.525	0.566	0.604
Energy interaction (kcal/mol)	-22.871	-21.805	-21.107	-20.288	-18.97	-18.37	-17.437	-16.948	-16.383
Energy Lennard-Jones (kcal/mol)	-22.116	-16.742	-15.737	-13.826	-9.544	-8.065	-6.878	-5.396	-3.97
Energy Coulomb (kcal/mol)	-0.601	-4.726	...	-6.324	-9.539	-10.613	-10.653	-11.66	-12.358
Pressure tensor Pzz (bar)	24519.7	2001.9	1086.8	6322.2	7444.2	4080.6	4828.5	4347.7	5376.6
$r_{CaO}$ first coordination shell (Å)	2.725	...	...	2.775	...	...	...	...	...
$g_{CaO}(r)$ coordination probability	7.504	...	...	7.774	...	...	...	...	...
$r_{CaO}$ second coordination shell (Å)	...	...	...	4.795	...	...	...	...	...
$g_{CaO}(r)$ coordination probability	1.524	...	...	1.615	...	...	...	...	...
$r_{CaO}$ third coordination shell (Å)	5.515	...	...	5.505	...	...	...	...	...
$g_{CaO}(r)$ coordination probability	1.543	...	...	1.461	...	...	...	...	...
Water O <sup>2-</sup> distance to midplane (Å)	0.012	...	-1.812	-1.612	...	...	...	...	...
"	...	0.012	-1.112	-0.537	...	...	...	...	...
"	...	...	0.087	0.587	...	...	...	...	...
"	...	...	1.262	1.687	...	...	...	...	...
"	...	...	1.562	1.124	...	...	...	...	...
O <sup>2-</sup> outmost layers separation (Å)	0	0	0	1.124	...	...	...	...	...
Water H <sup>+</sup> distance to midplane (Å)	-0.762	-0.862	-1.087	-1.087	...	-1.437	...	...	...
"	0.012	0.437	0.082	0.062	...	0.062	...	...	...
"	0.612	0.887	1.137	1.137	...	1.462	...	...	...
H <sup>+</sup> outmost layers separation (Å)	1.374	1.749	2.224	2.224	...	2.899	...	...	...
Ca <sup>2+</sup> distance to midplane (Å)	0.012	-0.787	-1.012	-1.012	...	-0.887	...	...	...
"	0.562	-0.237	-0.512	-0.512	...	0.912	...	...	...
"	...	0.912	0.537	0.537	...	1.262	...	...	...
"	...	...	1.112	1.112	...	...	...	...	...

Table 5. Monte Carlo simulation of hydrated Ca-montmorillonite,  $\mu$ VT ensemble, at 333 K and 300 bar.

Simulation	1	2	3	4	5	6	7	8
Temperature (K)	333	333	333	333	333	333	333	333
Pressure (bar)	300	300	300	300	300	300	300	300
Clay layers	2	2	2	2	2	2	2	2
Ca (atom/layer)	3	3	3	3	3	3	3	3
Water adsorbed (molecule/layer)	49.3	54.49	59.92	75.65	85.55	92.2	97.46	103.44
Water adsorbed (mg/g)	150.86	166.55	183.35	231.49	261.78	282.13	298.23	316.53
Spacing (Å)	12	12.5	13	14	14.5	15	15.5	16
Density (g/ml)	0.318	0.337	0.356	0.418	0.457	0.476	0.487	0.5
Energy interaction (kcal/mol)	-23.549	-22.803	-21.867	-20.795	-20.014	-19.673	-19.529	-19.11
Energy Lennard-Jones (kcal/mol)	-18.118	-6.345	-6.704	-9.073	...	-10.636	...	-11.396
Energy Coulomb (kcal/mol)	-5.647	-16.449	-14.937	-11.819	...	-8.884	...	-7.564
Pressure tensor Pzz (bar)	10654.69	-67.184	4179.982	5598.457	4137.781	2203.39	2539.388	2532.541
$r_{CaO}$ first coordination shell (Å)	...	2.804	...	...	...	...	...	...
$g_{CaO}(r)$ coordination probability	...	6.349	...	...	...	...	...	...
$r_{CaO}$ second coordination shell (Å)	...	4.725	...	...	...	...	...	...
$g_{CaO}(r)$ coordination probability	...	1.558	...	...	...	...	...	...
Water O <sup>2-</sup> distance to midplane (Å)	...	-1.812	...	...	...	...	...	...
"	...	-1.062	...	...	...	...	...	...
"	...	-0.012	...	...	...	...	...	...
"	...	1.192	...	...	...	...	...	...
Water H <sup>+</sup> distance to midplane (Å)	...	-1.812	...	...	...	...	...	...
"	...	-1.112	...	...	...	...	...	...
"	...	0	...	...	...	...	...	...
"	...	1.137	...	...	...	...	...	...
"	...	1.937	...	...	...	...	...	...
Ca <sup>2+</sup> distance to midplane (Å)	...	-0.812	...	...	...	...	...	...
"	...	0.587	...	...	...	...	...	...
"	...	1.137	...	...	...	...	...	...

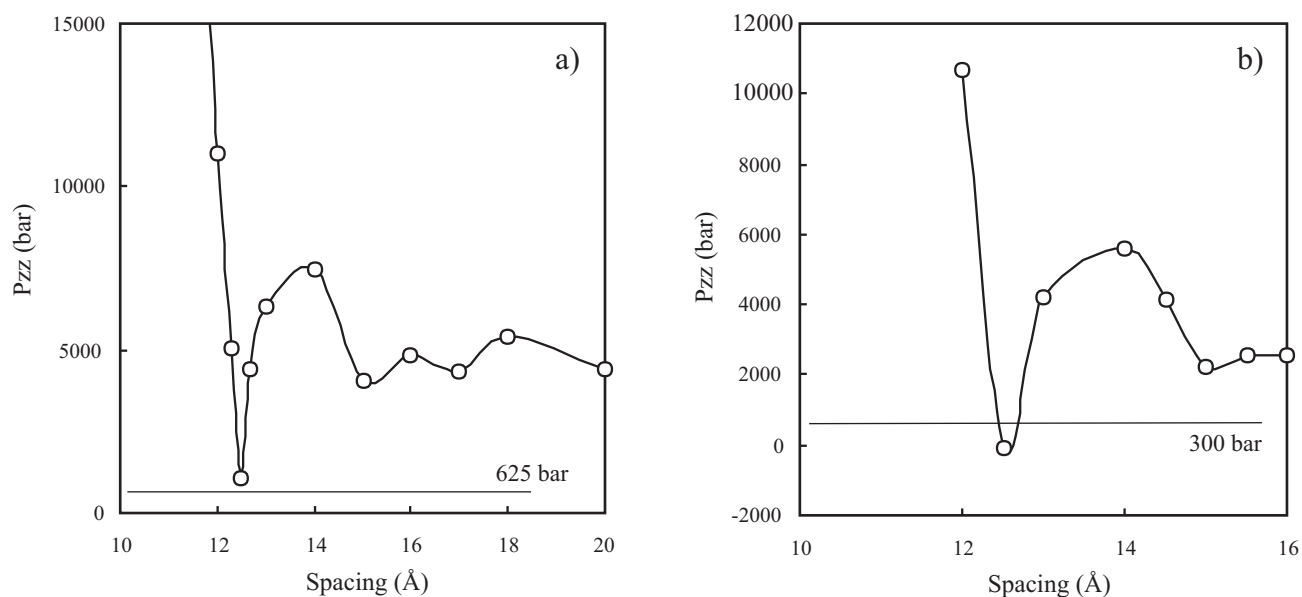


Figure 6. Variation of the pressure tensor  $P_{zz}$  with the  $d_{001}$  spacing, grand canonical  $\mu VT$  ensemble, at (a) 353 K, 625 bar, -5.88 kcal/mol, and (b) 333 K, 300 bar, -7.21 kcal/mol.

so their protons point towards the siloxane surfaces and the interlayer midplane. The calcium ions form outer-sphere complexes in the water layers, always positioned off the interlayer midplane.

For the force field considered in this work, within the statistical error of Monte Carlo simulations, Ca-montmorillonite forms a 12.11 Å one-layer hydrate stable at 333 K and 300 bar, at a 2 km depth of normally compacted sediments. Two- and three-layer hydrates do not form. At 353 K and 625 bar, prevailing at 2.7 km depth of over-compacted sedi-

ments, the one-layer hydrate only approaches stability without quite reaching it. Under equal conditions of temperature, pressure, and chemical potential our previous simulations indicate that Na-montmorillonite is clearly stable (de Pablo *et al.*, 2004) but K-montmorillonite may not (Chávez *et al.*, 2004). A difference is established with clays under the ambient surface setting of 300 K and 1 bar where two- and three-layer hydrates are formed. The results imply that Ca-montmorillonite as well as Na- and K-montmorillonite may, at depth, loose water to their one-layer hydrates.

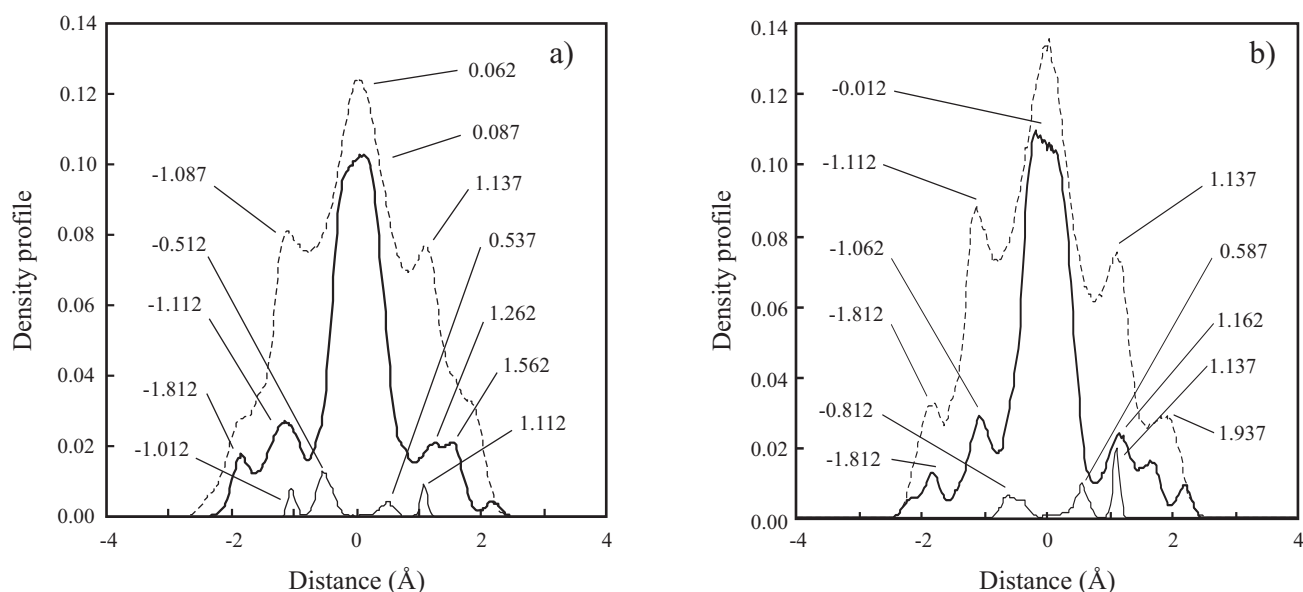


Figure 7. Density profiles of 1-layer Ca-montmorillonite hydrate, at (a) 353 K and 625 bar, (b) 333 K and 300 bar,  $\mu VT$  ensemble. Bold line: water oxygen; dashed: protons; black: calcium.

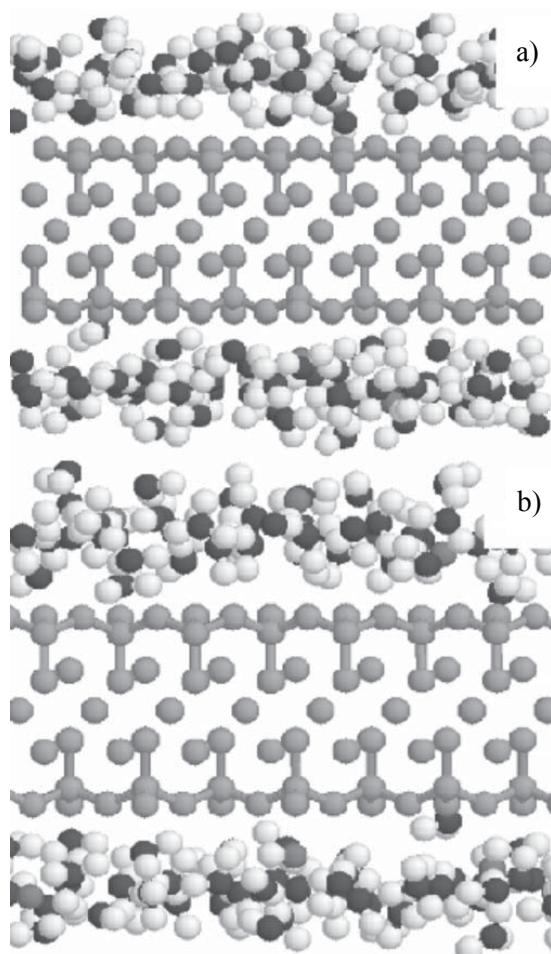


Figure 8. Snapshot of 1-layer Ca-montmorillonite at (a) 353 K and 625 bar, (b) 333 K and 300 bar, grand canonical ensemble.

## ACKNOWLEDGMENTS

The present study was supported by DGAPA, UNAM, Project IN106502. The authors thank DGSCA, UNAM, for extended allocation of their supercomputing resources. The Instituto Mexicano del Petroleo offered partial support.

## REFERENCES

Allen, M.P., Tildesley, D.J., 1987, *Computer Simulation of Liquids*: London, U.K., Clarendon Press, 404 p.  
 Anderson, M.A., Trouw, F.R., Tam, C.N., 1999, Properties of water in calcium- and hexadecyltrimethylammonium-exchanged bentonite: *Clays and Clay Minerals*, 47, 28-35.  
 Aylmore, L.A.G., Quirk, J.P., 1967, The micropore size distribution of clay mineral systems: *Journal of Soil Science*, 18, 1-17.  
 Boek, E.S., Coveney, P.V., Skipper, N.T., 1995, A study of hysteresis in the swelling curves of sodium montmorillonite: *Langmuir*, 11, 4629-4631.  
 Bounds, D.G. 1985, A molecular dynamics study of the structure of water around the ions  $\text{Li}^+$ ,  $\text{Na}^+$ ,  $\text{K}^+$ ,  $\text{Ca}^{2+}$ ,  $\text{Ni}^{2+}$ , and  $\text{Cl}^-$ : *Molecular Physics*, 54, 1335-1355.

Bray, H.J., Redfern, S.A.T., 1999, Kinetics of dehydration of Ca-montmorillonite: *Physics and Chemistry of Minerals*, 26, 591-600.  
 Bray, H.J., Redfern, S.A.T., 2000, Influence of counterion species on the dehydroxylation of  $\text{Ca}^{2+}$ ,  $\text{Mg}^{2+}$ ,  $\text{Na}^+$  and  $\text{K}^+$ -exchanged Wyoming montmorillonite: *Mineralogical Magazine*, 64, 337-346.  
 Bray, H.J., Redfern, S.A.T., Clark, S.M., 1998, The kinetics of dehydration in Ca-montmorillonite; An in-situ x-ray synchrotron study: *Mineralogical Magazine*, 62, 647-656.  
 Cases, M., Berend, I., François, M., Uriot, J.P., Michot, L.J., Thomas, F., 1997, Mechanism of adsorption and desorption of water vapor by homoionic montmorillonite. 3. The  $\text{Mg}^{2+}$ ,  $\text{Ca}^{2+}$ ,  $\text{Sr}^{2+}$ , and  $\text{Ba}^{2+}$  exchanged forms: *Clays and Clay Minerals*, 45, 8-22.  
 Chávez-Páez, M., de Pablo, L., de Pablo, J.J., 2001a, Monte Carlo simulations of Ca-montmorillonite hydrates: *Journal of Chemical Physics*, 114, 10948-10953.  
 Chávez-Páez, M., van Workum, K., de Pablo, L., de Pablo, J.J., 2001b, Monte Carlo simulations of sodium montmorillonite hydrates: *Journal of Chemical Physics*, 114, 1405-1413.  
 Chávez, M.L., de Pablo, L., de Pablo, J.J., 2004, Monte Carlo molecular simulation of the hydration of K-montmorillonite at 353 K and 625 bar: *Langmuir*, 20, 10764-10770.  
 Cotter-Howells, J.D., Patterson, E., 2000, Minerals and soil development, in Vaughan, D.J., Wogelius, R.A. (eds.), *Environmental Mineralogy*: Budapest, Eötvös University Press, 91-124.  
 De Pablo, L., Chávez, M.L., Sum, A.K., de Pablo, J.J., 2004, Monte Carlo molecular simulation of the hydration of Na-montmorillonite at reservoir conditions: *Journal of Chemical Physics*, 120, 939-946.  
 De Pablo, L., Chavez, M.L., de Pablo, J.J., 2005, Stability of Na-, K-, and Ca-montmorillonite at high temperatures and pressures; A Monte Carlo simulation: *Langmuir*, 21, 10874-10884.  
 Glaeser, R., Mering, J., 1968, Domaines d'hydratation homogène des smectites: *Comptes Rendus de l'Académie des Sciences (Paris)*, 267, Série D, 463-466.  
 Hall, P. L., 1993, Mechanism of overpressuring; an overview, in Manning, D.A.C., Hall, P.L., Hughes, C.R. (eds.), *Geochemistry of Clay-Pore Interactions*: London, U.K., Chapman and Hall, 265-315.  
 Hall, P. L., Astill, D. M., McConnell, J. D. C., 1986, Thermodynamic and structural aspects of the dehydration of smectites in sedimentary rocks, 21, 633-648.  
 Hower, J.E., Hower, M.E., Perry, E.A., 1976, Mechanism of burial metamorphism of argillaceous sediment; 1. Mineralogical and chemical evidence: *Geological Society of America Bulletin*, 86, 725-737.  
 Huggett, J.M., Shaw, H.F., 1993, Diagenesis of Jurassic mudrocks of the North Sea, in Manning, D.A.C., Hall, P.L., Hughes, C.R. (eds.), *Geochemistry of Clay-Pore Interactions*: London, U.K., Chapman and Hall, 107-126.  
 Jorgensen, W.L., Chandrasekhar, J., Madura, J.D., Impey, R.W., Klein, M.L., 1983, Comparison of simple potential functions for simulating liquid water: *Journal Chemical Physics*, 79, 926-935.  
 Keren, R., Shainberg, I., 1975, Water vapor isotherms and heat of immersion of Na/Ca-montmorillonite systems-I. Homoionic clay: *Clays and Clay Minerals*, 23, 193-200.  
 Khitarov, N.L., Pugin, V.A., 1996, Behavior of montmorillonite under elevated temperatures and pressures: *Geochemistry International*, 3, 621-626.  
 Koster von Groos, A.F., Guggenheim, S., 1987, Dehydration of a Ca-Mg-exchanged montmorillonite (SWy-1) at elevated pressures: *Clays and Clay Minerals*, 72, 292-298.  
 Koster von Groos, A.F., Guggenheim, S., 1989, Dehydroxylation of a Ca- and Mg-exchanged montmorillonite: *American Mineralogist*, 74, 627-636.  
 Laird, D.A., 1996, Model for the crystalline swelling of 2:1 layer phyllosilicates: *Clays and Clay Minerals*, 44, 553-559.  
 Laird, D.A., Shang, C., Thompson, M.L., 1995, Hysteresis in crystalline swelling of smectites: *Journal Colloid Interface Science*, 171,

240-245.

- McEwan, D.M.C., Wilson, M.J., 1980, Interlayer and intercalation complexes of clay minerals, *in* Brindley, G.W., Brown, G. (eds.), *Crystal Structures of Clay Minerals and their X-Ray Identification*: London, U. K., Mineralogical Society, 197-248.
- Pezerat, H., Mering, J., 1967, Recherches sur la position des cations échangeable et de l'eau dans les montmorillonite: *Comptes Rendus de l'Académie des Sciences (Paris), Série D*, 265, 529-532.
- Posner, A.M., Quirk, J.P., 1964, Changes in basal spacing of montmorillonite in electrode solution: *Journal of Colloidal Science*, 19, 798-812.
- Rutherford, D.W., Chiou, C.T., Eberl, D.D., 1980, Effects of exchanged cation on the microporosity of montmorillonite: *Clays and Clay Minerals*, 45, 534-543.
- Sato, T., Watanabe, T., Osuka, R., 1992, Effect of layer charge, charge location, and energy change on expansion properties of dioctahedral montmorillonites: *Clays and Clay Minerals*, 40, 103-113.
- Siqueira, A.V.C. de, Skipper, N.T., Coveney, P.V., Boek, E.S., 1997, Computer simulation evidence for enthalpy driven dehydration of smectite clays at elevated pressures and temperatures: *Molecular Physics*, 92, 1-6.
- Siqueira, A.V. de, Lobban, C., Skipper, N.T., Williams, G.D., Soper, A.K., Done, E., Dreyer, J.W., Humpreys, R.J.O., Bones, J.A.R., 1999, The structure of pore fluids in swelling clays at elevated pressures and temperatures: *Journal of Physical Condensed Matter*, 11, 9179-9188.
- Skipper, N.T., Sposito, G., Chang, F.R.C., 1995a, Monte Carlo simulation of interlayer molecular structure in swelling clay minerals. 2. Monolayer hydrates: *Clays and Clay Minerals*, 43, 294-303.
- Skipper, N.T., Chang, F.R.C., Sposito, G., 1995b, Monte Carlo simulation of interlayer molecular structure in swelling clay minerals. 1. Methodology: *Clays and Clay Minerals*, 43, 285-293.
- Slade, P.G., Quirk, J.P., Norrish, K., 1991, Crystalline swelling of smectite samples in concentrated NaCl solutions in relation to layer charge: *Clays and Clay Minerals*, 39, 234-238.
- Stone, R.L., Rowland, R.A., 1955, DTA of kaolinite and montmorillonite under H<sub>2</sub>O vapor pressure up to six atmospheres, *in* Third National Clay Conference of the Clay Minerals Society: Houston, Texas, National Academy of Sciences and National Research Council, 39, 103-116.
- Suquet, H., de la Calle, C., Pezerat, H., 1975, Swelling and structural properties of saponite: *Clay and Clay Minerals*, 23, 1-9.
- Wu, T.C., Bassett, W.A., Huang, H.L., Guggenheim, S., Koster van Groos, A.F. 1997, Montmorillonite under high H<sub>2</sub>O pressures: Stability of hydrated phases, dehydration hysteresis, and the effect of interlayer cations: *American Mineralogist*, 82, 69-78.

Manuscript received: May 10, 2005

Corrected manuscript received: October 4, 2005

Manuscript accepted: November 18, 2005